

# Dynamic Behaviour of Cast A356/Al<sub>2</sub>O<sub>3</sub> Aluminum Metal Matrix Nanocomposites

El-Sayed Youssef El-Kady, Tamer Samir Mahmoud, Ahmed Abdel-Fattah El-Betar,  
Mohamed Abdel-Aziz Sayed

Mechanical Engineering Department, Faculty of Mechanical Engineering, King Khalid University, Abha, KSA.  
Email: Eyselkay@yahoo.com

Received June 2<sup>nd</sup>, 2012; revised July 19<sup>th</sup>, 2012; accepted September 14<sup>th</sup>, 2012

## ABSTRACT

The present work includes the study of the dynamic properties of the nanocomposites specimens. The dynamic properties of A356/Al<sub>2</sub>O<sub>3</sub> nanocomposites were investigated through different fabrication conditions. The A356/Al<sub>2</sub>O<sub>3</sub> nanocomposites specimens were fabricated using a combination between the rheocasting and squeeze casting routes. The composites were reinforced with Al<sub>2</sub>O<sub>3</sub> particulates of 60 and 200 nm and different volume fractions up to 5 vol%. The dynamic properties of the A356/Al<sub>2</sub>O<sub>3</sub> nanocomposites were investigated through measuring the dynamic properties of specimens. Free vibration method is used to measure frequency response ( $f_n$ ), and damping factor ( $\zeta$ ). The viscoelastic properties such as loss factor  $\eta$ , storage modulus ( $E'$ ), and loss modulus ( $E''$ ) were obtained. The results concluded that, the dynamic properties of nanocomposites were improved by increasing the volume fractions of nanoparticulates and decreasing the nanoparticulates size. The results indicated also that, the damping factor, and the related parameters ( $\eta$ ,  $E'$  and  $E''$ ) was strongly affected by increasing both volume fraction and the particulates.

**Keywords:** Metal Matrix Nanocomposites; Aluminum Alloys; Dynamic Properties; Damping Factor; Vibration; Frequency; Stiffness; Loss Factor; Storage Modulus

## 1. Introduction

In aerospace and many other lightweight structures, there are many vibration inputs that can lead to resonance, so it is necessary to have a sound methodology to control the vibration. During the past few decades, it has become technically and ecologically important to suppress vibration and impact noise [1,2]. From this scope, many mechanical dampers have been investigated and developed and there, the exploitation of damping materials is a key point to produce efficient damping to eliminate vibration and noise [3]. Damping materials have good ability to dissipate elastic strain energy when subjected to vibratory loads and have been widely used in the fields of high performance structural applications such as aerospace, marine, construction, etc. Damping is an important modal parameter for the design of structures for which vibration control and cyclic loading are critical. Damping is also a significant factor for the fatigue life and impact resistance of structures. Damping varies with different environmental effects, such as frequency, amplitude of stress, temperature and static preload. Damping is also affected by corrosion fatigue, grain size, porosity and number of fatigue cycles, especially for metallic materials [4].

Metal matrix composites (MMCs) have attracted great

attention in automotive and aerospace industries due to their high tensile and fatigue strengths, modulus of elasticity, higher micro-plastic strain resistance, adjustable heat conductivity and thermal expansibility [5]. MMC consists of a metallic base with a reinforcing constituent, usually ceramic. Normally, micro-sized ceramic particles are used to improve the yield and ultimate strength of the metal. However, the ductility of the MMCs deteriorates with high ceramic particle concentration [1]. Recently, it is of interest to use nano-sized ceramic particles to strengthen the metal matrix, so-called metal matrix nano-composite (MMNC), while maintaining good ductility [6,7]. With nanoparticulates reinforcement, especially high temperature creep resistance and better fatigue life could be achieved. Nowadays, interest is growing in producing composites reinforced by nanoparticulates either by adding these particulates to liquid metals or by in situ techniques. Many researches [8,9] have claimed enhanced properties for the produced composites relative to those produced by reinforcing with the micro-particles.

Few investigations were reported on the dynamic properties of metal matrix nanocomposites (MMNCs). For example, Deng *et al.* [10] studied the damping characteristics of 2024 Al alloy reinforced with multi-walled carbon nanotube (MWNTs) fabricated by a procedure of

mixing 2024 Al powders and CNTs, cold isostatic press and hot extrusion. The damping behaviors of the composite were investigated with frequency of 0.5, 1.0, 5.0, 10, 30 Hz, at a temperature of 25°C - 400°C. The experimental results show that the frequency significantly affects the damping capacity of the composite when the temperature is above 230°C; meanwhile, the damping capacity of the composite with a frequency of 0.5 Hz reaches  $9.75 \times 10^{-1}$ , and the storage modulus is 82.3 GPa when the temperature is 400°C, which shows that CNTs are a promising reinforcement for metal matrix composites to obtain high damping capabilities at an elevated temperature without sacrificing the mechanical strength and stiffness of a metal matrix.

In the present investigation, the dynamic properties of the A356/Al<sub>2</sub>O<sub>3</sub> nanocomposites were studied. The effect of dispersion of Al<sub>2</sub>O<sub>3</sub> nanoparticulates into A356 aluminum alloy on the natural frequency, damping factor, stiffness, storage modulus and loss modulus were investigated.

## 2. Experimental Procedures

The A356 Al-Si-Mg cast alloy was used as a matrix. The chemical composition of the A356 Al alloy is listed in **Table 1**. Nano-Al<sub>2</sub>O<sub>3</sub> particulates were used as reinforcing agents. The Al<sub>2</sub>O<sub>3</sub> nanoparticulates have two different average sizes, typically, 200 and 60 nm. Several metal matrix nanocomposites (MMNCs) were fabricated with different volume fractions of Al<sub>2</sub>O<sub>3</sub> nanoparticulates up to 5 vol%.

The A356/Al<sub>2</sub>O<sub>3</sub> nanocomposites were prepared using a combination of rheocasting and squeeze casting techniques. Preparation of the composite alloy was carried out according to the following procedures: About 1 kg of the A356 Al alloy was melted at  $680^\circ\text{C} \pm 2^\circ\text{C}$  in a graphite crucible in an electrical resistance furnace. After complete melting and degassing by argon gas of the alloy, the alloy was allowed to cool to the semisolid temperature of 602°C. At such temperature the liquid/solid fraction was about 0.7. The liquid/solid ratio was determined using primarily differential scanning calorimeter (DSC) experiments performed on the A356 alloy. A simple mechanical stirrer with three blades made from stainless steel coated with bentonite clay was introduced into the melt and stirring was started at approximately 1000 rpm. Before stirring the nanoparticulates reinforcements after heating to 400°C for two hours were added inside the vortex formed due to stirring. After that, preheated Al<sub>2</sub>O<sub>3</sub>

nanoparticulates were introduced into the matrix during the agitation. After completing the addition of Al<sub>2</sub>O<sub>3</sub> nanoparticulates, the agitation was stopped and the mixture was poured into preheated tool steel mould and immediately squeezed during solidification. The produced ingot has 30 mm diameter and  $130 \pm 10$  mm length. The nanocomposites were heat treated at T6 before conducting the machining tests.

Samples from the fabricated composites were cut from the cast ingot for microstructural examinations. Specimens were ground under water on a rotating disc using silicon carbide abrasive discs of increasing finesse up to 1200 grit. Then they were polished using 10 µm alumina paste and 3 µm diamond paste. Microstructural examinations were conducted using both optical and scanning electron microscopes (SEM). Microstructural examination was performed in the unetched condition. The porosity of the nanocomposites was measured using the typical Archimedes (water displacement) method.

Rectangular specimens having 100 mm of length, 20 mm of width and 1.5 mm of thickness shown schematically in **Figure 1** were longitudinally cut from the cast nanocomposites ingots.

The damping factor and natural frequency are measured experimentally using vibration testing equipment (see **Figure 2**) containing an accelerometer, (type 4394

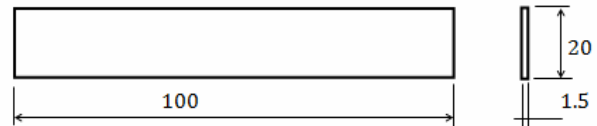


**Figure 1.** A schematic illustration of the specimens.

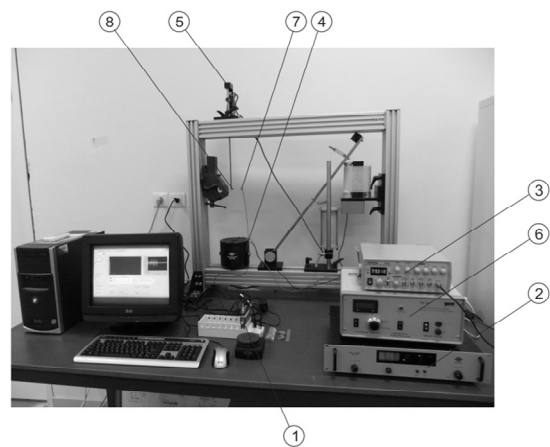


**Figure 2.** Test rig and the equipment used in experimental work. (1) NI DAQ-9172, (2) Power amplifier-type 2718 (B&K), (3) Pintek function generator FG32, (4) Drives vibration exciter type 4809, (5) Force exciter (Gunt), (6) Electronic control unit (Gunt exciter) for precise regulation and display of excitation frequency, (7) Vibration sensor (accelerometer type 4394 B&K), (8) Specimen.

**Table 1.** Chemical composition (wt%) of the A356 alloy.

Si	Fe	Cu	Mn	Mg	Zn	Al
6.6	0.25	0.11	0.002	0.14	0.026	Bal.

B&K), exciter, (exciter type 4809 + Power Amplifier-Type 2718 (from B&K) + Pintek function generator G32) or (Gunt exciter + Frequency control unit), Data Acquisition (NI DAQ-9172), and vibration analyses software (LabView) and a computer to display the analysis result. In this equipment, the specimen is attached to cantilever configuration. The vibration test gives the free vibration damping decay and the frequency response function (FRF), simultaneously as a result. Considering a linear system of a single degree of freedom, the FRF response is the decomposition of the natural frequencies of a structure or specimen which corresponds to a typical fingerprint identify of the vibration modes. The number of vibration peak frequencies (vibration mode) and the shape of the FRF response are a direct result of the rigidity of the material. The amplitude decay was measured using a 2.7 g accelerometer.

### 3. Results and Discussion

#### 3.1. Microstructural Examinations

**Figure 3** shows example micrographs of the microstructure of the monolithic A356 alloy as well as the A356/Al<sub>2</sub>O<sub>3</sub> nanocomposites after heat treatment. It is clear from **Figure 3(a)** that the structure of the monolithic A356 Al alloy consists of primary  $\alpha$  phase (white regions) and Al-Si eutectic structure (darker regions). Needle-like primary Si particulates were found to be distributed along the boundaries of the  $\alpha$ -Al dendrites. **Figures 3(b)** and **3(c)** show micrographs of nanocomposites containing 3 vol% of Al<sub>2</sub>O<sub>3</sub> nanoparticulates having 60 and 200 nm, respectively. Clusters of nanoparticulates in the microstructure of the A356/Al<sub>2</sub>O<sub>3</sub> nanocomposite were observed. **Figure 3(d)** shows high magnification micrograph of Al<sub>2</sub>O<sub>3</sub>/5 vol% (200 nm) nanocomposites. It is clear that clusters of nanoparticulates clusters are located inside the  $\alpha$ -grains as well as near the eutectic structure. **Figure 4(a)** shows high magnification SEM micrograph of the 5 vol% Al<sub>2</sub>O<sub>3</sub> nanoparticulates (200 nm) showing that nanoparticulates are agglomerating near the Si particles of the eutectic structure. The XRD analysis for the nanoparticulates is shown in **Figure 4(b)**. Also, it has been observed that increasing the volume fraction of the nanoparticulates dispersed inside the A356 alloy increases the agglomeration percent. The nanocomposites containing 5 vol% exhibited the highest agglomeration percent when compared with those containing 1 and 3 vol%.

Porosity measurements indicated that the nanocomposites have porosity content lower than 2 vol%. Such low porosity content is attributed to the squeezing process that carried out during the solidification of the nanocomposites. In cast MMCs, there are several sources of gases. The occurrence of porosity can be attributed vari-

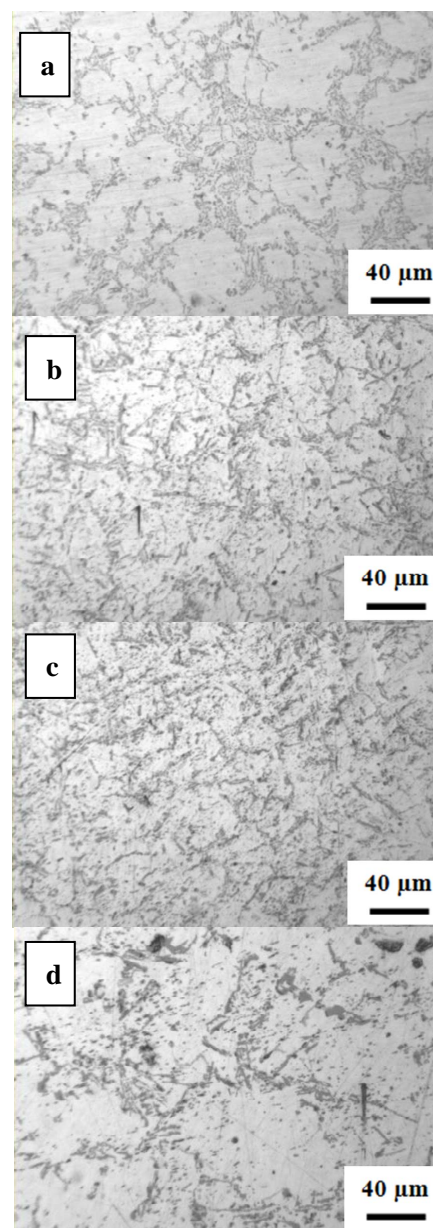
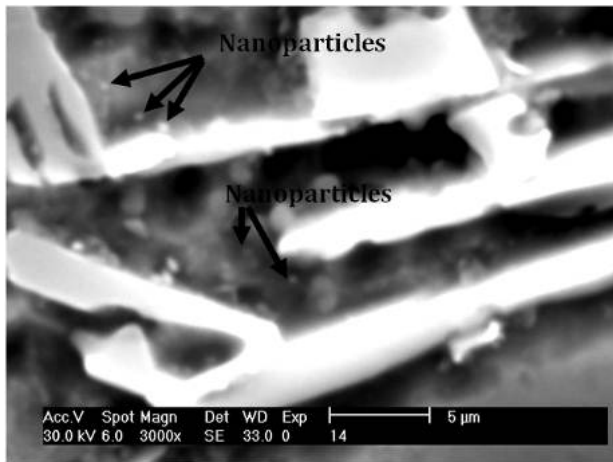


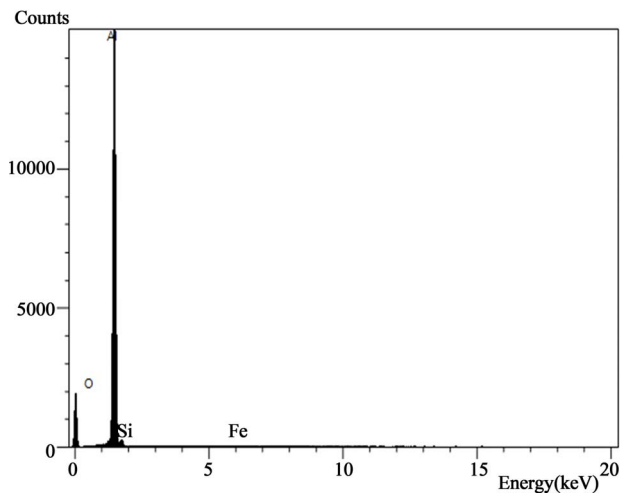
**Figure 3.** Optical micrographs for (a) A356 monolithic alloy; (b) A356: 3 vol% Al<sub>2</sub>O<sub>3</sub> (60 nm) nanocomposites; (c) A356: 3 vol% Al<sub>2</sub>O<sub>3</sub> (200 nm) nanocomposites; (d) A356: 5 vol% Al<sub>2</sub>O<sub>3</sub> (200 nm) nanocomposites.

ously to the amount of hydrogen gas present in the melt, the oxide film on the surface of the melt that can be drawn into it at any stage of stirring, and the gas being drawn into the melt by certain stirring methods [5]. Vigorously stirred melt or vortex tends to entrap gas and draw it into the melt. Increasing the stirring time allows more gases to be entered into the melt and hence reduce the mechanical properties.

The amount of liquid inside the semi-solid slurry increases with increasing the temperature which on the other hand reduces the viscosity of the solid/liquid slurry.



(a)



(b)

**Figure 4.** (a) High magnification SEM micrograph of the 5 vol% Al<sub>2</sub>O<sub>3</sub> nanoparticles (200 nm) showing that nanoparticles are agglomerating near the Si particles of the eutectic structure; (b) XRD analysis for the particles shown in (a).

Nanoparticulates distribution in the A356 Al matrix alloy during the squeezing process depends greatly on the viscosity of the slurry and also on the characteristics of the reinforcement particles themselves, which influence the effectiveness of squeezing in to break up agglomerates and distribute particles. When the amount of liquid inside the slurry is large enough, the particles can be rolled or slid over each other and thus breaking up agglomerations and helping the redistribution of nanoparticulates and improving the microstructure.

### 3.2. Dynamic Behaviour of Nanocomposites

**Figure 5** and **Table 2** present the resonant frequency  $f_n$  results and damping factor  $\zeta$  of all specimens studied in the current work. The first mode of vibration and the damping factor was used in order to calculate the  $E'$  and  $E''$  moduli and loss factor  $\eta$ . **Table 2** shows the response of the natural frequency of the nanocomposites. It can be observed that both the natural frequency and the damping factor increase with increasing of volume fraction and/or decreasing the Al<sub>2</sub>O<sub>3</sub> nanoparticulates size.

The obtained results revealed that the damping factor of nanocomposites relative to the matrix alloy specimens were increased by factor 2%, 3% and 4% when the volume fraction of composites are 1, 3 and 5 vol% respectively. The obtained results indicated also that the decreasing of particulates size from 200 to 60 nm was increased the damping factor by an approximately value of 1.7% from that obtained for the composites having the same volume fraction. Similar trends of results were also noticed for storage modulus, loss factor and loss modulus as shown in **Table 2**.

The effects of volume fractions on damping factor were related to the reinforcement particulates absorbing the external forces through broking the continuity of line of working force, then increasing the length of force working line so, reduces the effect of external force and

**Table 2.** Dynamic characteristics of A356/Al<sub>2</sub>O<sub>3</sub> nanocomposite.

No.	Material	Al <sub>2</sub> O <sub>3</sub> Additive			Dynamic Properties			
		Size (nm)	Volume Fraction vol%	Damping Factor $\zeta$	Natural Frequency $f_n$ , Hz	Storage Modulus $E'$ , GPa	Loss Factor $\eta$	Loss Modulus $E''$ , GPa
1		0	0	0.003	18.6	3.350	0.006	0.020
2		200	1 %	0.006	22.0	5.122	0.012	0.061
3		200	3 %	0.009	27.0	7.058	0.018	0.127
4	A356/Al <sub>2</sub> O <sub>3</sub>	200	5 %	0.011	41.0	16.270	0.022	0.358
5		60	1 %	0.013	24.0	5.400	0.026	0.140
6		60	3 %	0.015	42.8	17.738	0.030	0.532
7		60	5 %	0.018	68.0	44.760	0.036	1.611

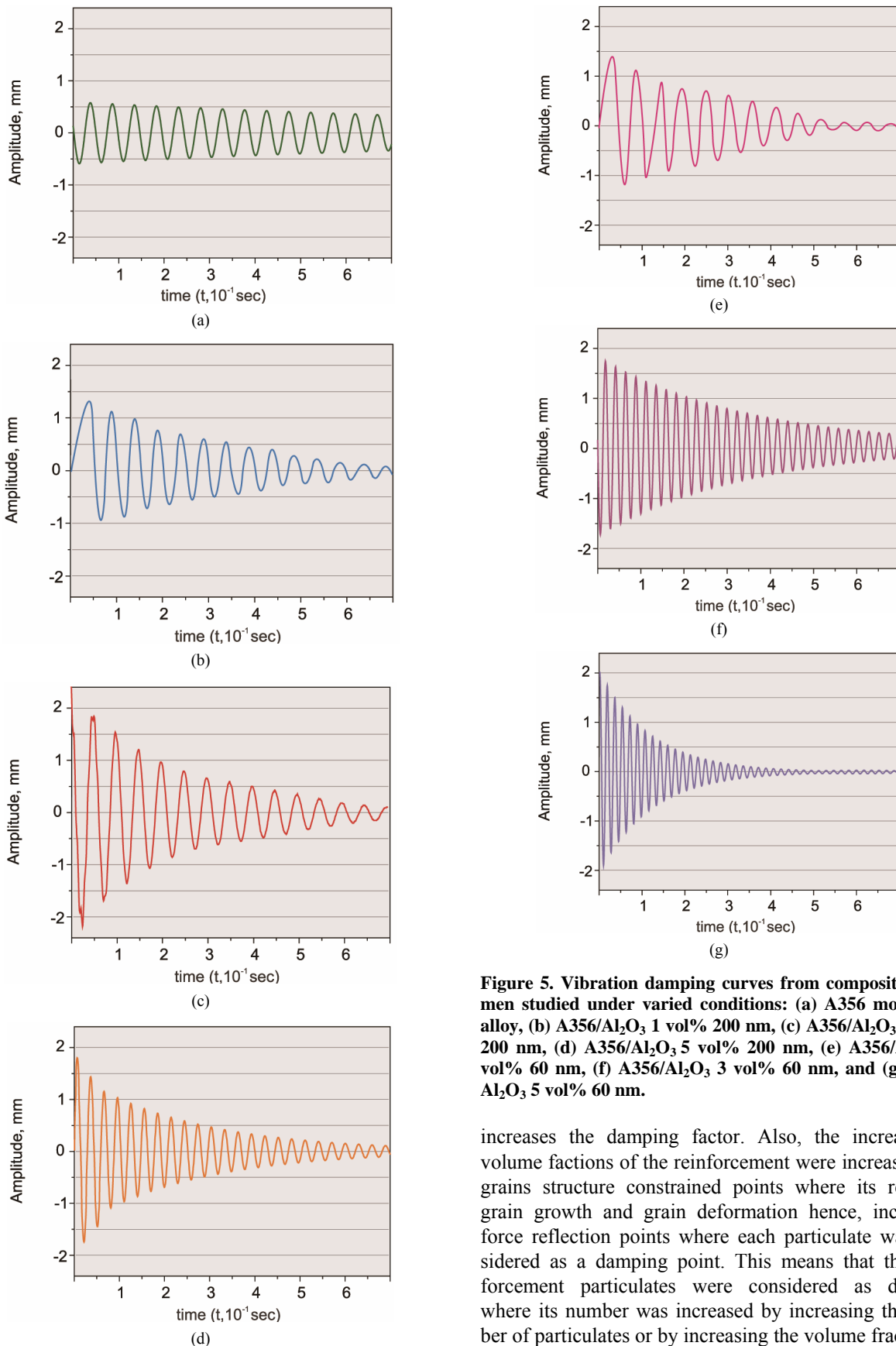


**Figure 5. Vibration damping curves from composite specimen studied under varied conditions: (a) A356 monolithic alloy, (b) A356/Al<sub>2</sub>O<sub>3</sub> 1 vol% 200 nm, (c) A356/Al<sub>2</sub>O<sub>3</sub> 3 vol% 200 nm, (d) A356/Al<sub>2</sub>O<sub>3</sub> 5 vol% 200 nm, (e) A356/Al<sub>2</sub>O<sub>3</sub> 1 vol% 60 nm, (f) A356/Al<sub>2</sub>O<sub>3</sub> 3 vol% 60 nm, and (g) A356/Al<sub>2</sub>O<sub>3</sub> 5 vol% 60 nm.**

increases the damping factor. Also, the increases of volume fractions of the reinforcement were increasing the grains structure constrained points where its resisting grain growth and grain deformation hence, increasing force reflection points where each particulate was considered as a damping point. This means that the reinforcement particulates were considered as dampers where its number was increased by increasing the number of particulates or by increasing the volume fraction of

the reinforcement. Therefore, it may be concluded that the increases of volume fraction of the reinforcement particulates were increasing the damping points, so increasing the damping factor.

The effect of the nanoparticulates size on the natural frequency of composites was noticed in results shown in **Table 2** and **Figures 5(e)-(g)**. These results show that the natural frequency of composites having small particulates size (60 nm) more than that of larger particulates size (200 nm). These results due to the decrease of particulates size were increasing both composites strength and ductility as concluded in the previous work conducted by El-Kady *et al.* [9], hence increasing stiffness and natural frequency. Similar results were obtained when calculating the storage modulus, loss factor and loss modulus, where these parameters were strongly affected by increasing volume fraction or decreasing particulates size as discussed before where the effects were subject to the same reasons which effects on damping factor and natural frequency.

#### 4. Conclusions

In the present study, experimental work was employed to determine dynamic behaviors of nanocomposite material. The Effect of volume fraction and particular size of nano additives on the natural frequency, damping factor, storage modulus, loss modulus and loss factor was analyzed for the A356/Al<sub>2</sub>O<sub>3</sub> reinforced nanocomposite which prepared using a combination of rheocasting and squeeze casting techniques compared to the A356 alloy. The vibration testing response proved to be an effective tool for measuring the damping properties of nanocomposites.

The influence of the Al<sub>2</sub>O<sub>3</sub> nanoparticulates size and volume fraction on the natural frequency, damping factor, storage modulus, loss modulus, and loss factor was found experimentally. It was found that by increasing the reinforcement volume fraction the natural frequency, damping factor, storage modulus, loss modulus, and loss factor increase. The results also indicate that decreasing the Al<sub>2</sub>O<sub>3</sub> nanoparticulates size enhances the natural frequency, damping factor, storage modulus, loss modulus, and loss factor of the nanocomposites.

#### 5. Acknowledgements

This work is supported by the King Abdel-Aziz City of Science and Technology (KACST) through the Science and Technology Center at King Khalid University (KKU), Fund (NAN 08-172-07). The authors thank both KACST and KKU for their financial support. Special Thanks to Prof. Dr. Ahmed Taher, Vice President of KKU, Prof. Dr. Eid Al-Atibi, Dean of the Scientific Re-

search at KKU, Prof. Dr. Abdullah Al-Sihimi Director of the research center of Excellency at KKU and Dean of the faculty of Science and finally great thanks to Dr. Khaled Al-Zailaie, Dean of the faculty of engineering at KKU, for their support.

#### REFERENCES

- [1] ASM Handbook, "Composites," Vol. 21, 2001.
- [2] D. Zhang and D. Jia, "Toughness and Strength Improvement of Diglycidyl Ether of Bisphenol-A by Low Viscosity Liquid Hyperbranched Epoxy Resin," *Journal of Applied Polymer Science*, Vol. 101, No. 4, 2006, pp. 2504-2511. doi:10.1002/app.23760
- [3] R. C. Cabanelas, B. Serrano and I. Baselga, "Development of Co Continuous Morphologies in Initially Heterogeneous Thermosets Blended with Poly(Methyl Methacrylate)," *Macromolecules*, Vol. 38, No. 3, 2006, pp. 961-970. doi:10.1021/ma0487352
- [4] M. Colakoglu, "Factors Effecting Internal Damping in Aluminum," *Theory of Applied Mechanics*, Vol. 42, No. 1, 2004, pp. 95-105.
- [5] I. S. El-Mahallawi, K. Eigenfield, F. Kouta, A. Hussein, T. S. Mahmoud, R. M. Ragaie, A. Y. Shash and W. Abou-Al-Hassan, "Synthesis and Characterization of New Cast A356/(Al<sub>2</sub>O<sub>3</sub>)<sub>p</sub> Metal Matrix Nanocomposites," *The Proceeding of the ASME 2nd Multifunctional Nanocomposites & Nanomaterials: International Conference & Exhibition*, Cairo, 11-13 January 2008.
- [6] Y. Yang, J. Lan and X. C. Li, "Study on Bulk Aluminum Matrix Nanocomposite Fabricated by Ultrasonic Dispersion of Nano-Sized SiC Particles in Molten Aluminum Alloy," *Materials Science & Engineering A*, Vol. 380, No. 1-2, 2004, pp. 378-383. doi:10.1016/j.msea.2004.03.073
- [7] X. L. Zhong, W. L. E. Wong and M. Gupta, "Enhancing Strength and Ductility of Magnesium by Integrating it with Aluminum Nanoparticles," *Acta Materialia*, Vol. 55, No. 18, 2007, pp. 6338-6344. doi:10.1016/j.actamat.2007.07.039
- [8] E. Y. El-Kady, T. S. Mahmoud and A. A. Ali, "On the Electrical and Thermal Conductivities of Cast A356/Al<sub>2</sub>O<sub>3</sub> Metal Matrix Nanocomposites," *Materials Sciences and Applications*, Vol. 2, No. 9, 2011, pp. 1180-1187. doi:10.4236/msa.2011.29159
- [9] E. Y. El-Kady, T. S. Mahmoud and M. Abdel-Aziz Sayed, "Elevated Temperatures Tensile Characteristics of Cast A356/Al<sub>2</sub>O<sub>3</sub> Nanocomposites Fabricated Using a Combination of Rheocasting and Squeeze Casting Techniques," *Materials Sciences and Applications*, Vol. 2, No. 5, 2011, pp. 390-398. doi:10.4236/msa.2011.25050
- [10] C. F. Deng, D. Z. Wang, X. X. Zhang and Y. X. Ma, "Damping Characteristics of Carbon Nan Tube Reinforced Aluminum Composite," *Materials Letters*, Vol. 61, No. 14-15, 2007, pp. 3229-3231. doi:10.1016/j.matlet.2006.11.073